GEOPHYSICS, VOL. 37, NO. 2 (APRIL 1972), P. 351–374, 26 FIGS., 1 TABLE

ELECTROMAGNETIC DEPTH SOUNDING EXPERIMENT ACROSS SANTA CLARA VALLEY†

JISOO RYU*, H. FRANK MORRISON‡, AND STANLEY H. WARD*

An electromagnetic depth sounding experiment with a horizontal loop carrying an oscillating current was carried out in Santa Clara Valley, California. The field data are interpreted in terms of the polarization parameters of the magnetic polarization ellipse. The chosen parameters are tilt-angle, ellipticity, and the modulus of wave-tilt. The electrical discontinuities deduced are in general agreement with well data and with a geologic section based on resistivity soundings. The results clearly reveal an intermediate, highly resistive layer, which is a permeable stratum for groundwater recharge. It is concluded that a portable electromagnetic sounding system, measuring only tilt-angle and ellipticity, should easily locate highly resistive gravel deposits bounded by conductive clay beds. It is theoretically obvious that the system is useful in those regions where it is extremely difficult to inject current into the ground.

INTRODUCTION

The primary objective of the subject experiment is to investigate the capability of an active electromagnetic sounding system, with a horizontal loop carrying an oscillating current (Ie^{iwt}), to define electrically layered structures and thicknesses of unconsolidated sediments. The experimental results serve as a practical test of the theoretical conclusions of our earlier paper (Ryu et al, 1970).

Conventional resistivity soundings and induced-polarization methods have been utilized successfully to study ground water and related problems (Vacquier et al, 1957; Breusse, 1963; Zohdy, 1964; Sumi, 1965; Bodmer et al, 1968; and others). These static electrical methods may not be useful over those areas where it is extremely difficult to inject current into the ground. It was thought that the electromagnetic sounding system might serve the same purposes as the static systems and overcome some of the difficulties encountered with the static electrical methods.

The theory of electromagnetic sounding methods has been developed (Keller and Frischknecht, 1966; Vanyan, 1967; Dey and Ward, 1970; Ryu et al, 1970; and others), and the complexity of the problem has been demonstrated, but little has been written on the engineering and hydrological applications of the electromagnetic sounding method. To mention a few examples of the sounding experiments, Patra (1967) used central induction sounding in *parametric* mode for measuring water table depths; Inouye et al (1969) carried out a survey with a two-coil tilt-angle electromagnetic system. In 1962, F. C. Frischknecht and L. A. Anderson (Frischknecht, 1967) made a depth sounding on the Kilauea Iki Lava Lake, Hawaii to determine the thickness of the upper solidified lava. The feasibility of the inductive induced-polarization method was field tested with the electromagnetic sounding system by Hohmann et al (1970). Duckworth (1970) suggested a simplified approach to electromagnetic depth sounding, in the *geometric mode*, for mining purposes.

The present experiment was designed to detect clay, sand, clayey sand, or gravel horizons

† Manuscript received by the Editor June 8, 1971; revised manuscript received October 13, 1971.

* University of Utah, Salt Lake City, Utah 84112.

‡ University of California, Berkeley, California 94704

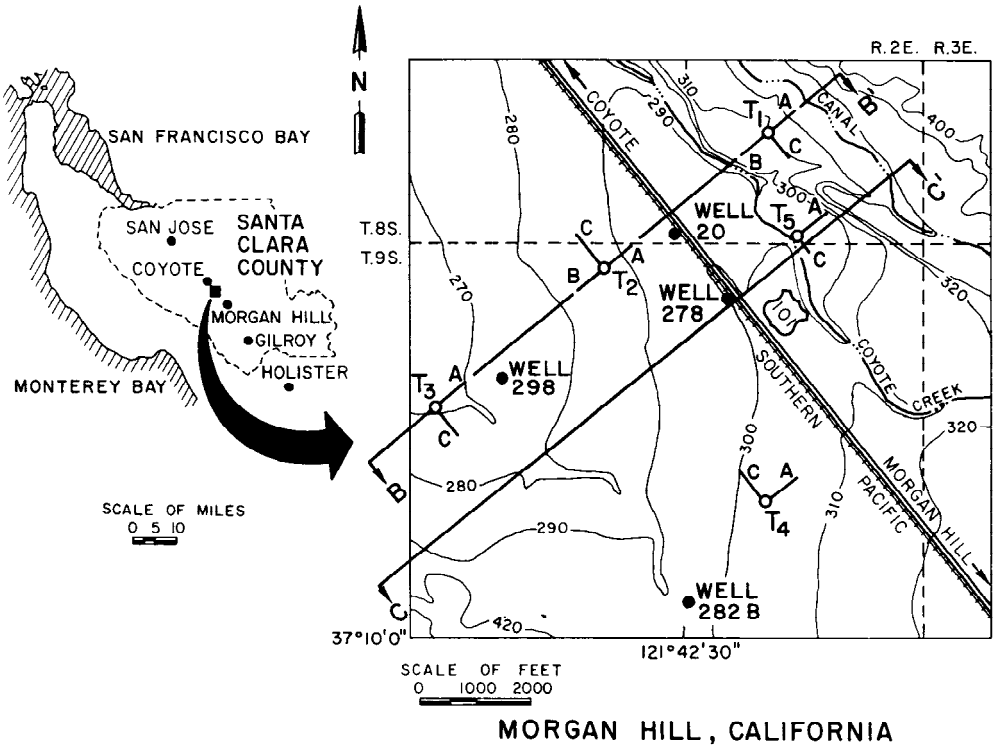

FIG. 1. Location of surveyed area and detailed location of transmitter sites.

within a few hundred meters of the earth's surface and to yield the possible locations of natural groundwater reservoirs occuring in unconsolidated sediments. The results of the present experiments should pertain in principle to the following problems: identifying and/or remote monitoring the depth of groundwater table; determining the thicknesses and depths of subsurface stratification of sediments, minerals, or rocks; mapping ice occurrences and thicknesses in permafrost and marine environments; detecting the intrusion of salt water along shorelines; and studying lunar and planetary environments.

LOCATION AND GEOLOGIC SETTINGS OF SURVEYED AREA

The electromagnetic depth sounding experiment was carried out across the lower part of Santa Clara Valley, as shown in the map of Figure 1, about 14 miles south of the city of San Jose, between Coyote and Morgan Hill. The valley developed between the Santa Cruz Mountains and the Mount Hamilton Range. The detailed locations of five transmitter sites are also shown in Figure 1, designated by $T_i (i = 1, 5)$. Each location has two or three receiver lines, labelled A, B, and C. The transmitter sites T_1, T_2, and T_3 were laid out to obtain an electrical structure across the valley while T_4 and T_5 were laid out to cross-check responses with those at T_2 and T_1, respectively.

A representative geologic column of the Morgan Hill quadrangle and the aerial distribution of the geologic formations of Santa Clara Valley around the field site (Hill, 1955) are shown in Figures 2 and 3, respectively.

The geology of the Santa Clara Valley was described in detail by Poland and Green (1962). The bedrock ranges in age from upper Jurassic to Pliocene. It consists mainly of consolidated sedimentary rocks, but igneous and metamorphic rocks are also exposed in some areas. Underlying the unconsolidated alluvial deposit, the bedrock is packwood gravels of Pliocene and Pleistocene age and consists of poorly sorted, cross-bedded conglomerate, sandstone, mudstone, marl, and

some limestone with interbedded tuff and basalt near base. From the structural point of view, the Santa Clara Valley is essentially a graben type of structure filled with unconsolidated sediment. Upper unconsolidated alluvial and bay deposits of clay, sand, and gravel are of interest in our experiment. The existing well data around the field site were supplied by the Water Conservation District, Santa Clara Valley and are given in Figure 4. It is reported that the alluvial and bay deposits might reach thicknesses of 1000 ft in the valley trough.

INSTRUMENTATION

The block diagram of the electromagnetic frequency sounding system is sketched in Figure 5. The selection of equipment was partly dictated by availability within our budgetary limit.

The transmitting loop has a radius of 10 m, with twenty turns of no. 10 copper wire. It was driven by a model 14094 audio power amplifier manufactured by Tel-Instrument Electronics Corp., and was loaned to the experiment by the U. S. Navy. This audio power amplifier has a rated output of 10 kva over a frequency range of 200 hz to 15,000 hz and requires an input power of approximately 30 kva at a full rated output. The transmitting loop has a resistance of about 4 ohms, which is the minimum output load of the amplifier. It is series tuned to maximize the output current and minimize the signal distortion. The frequency of the input sine-wave was accurately recorded with a digital frequency counter.

The transmitted signal was detected by a calibrated, ferrite-cored coil, which has a diameter of 12.5 cm and consists of 12,000 turns of no. 36 wire. The detected signal was then passed through a low noise Par CR-4 preamplifier and a Krohn-Hite model 3222 bandpass filter, and monitored on an ac voltmeter. When necessary, the signal was also monitored on an oscilloscope. All of the receiving units were battery operated. Both the coil and the bandpass filter were supplied by Kennecott Exploration Services, Inc.

It was difficult to measure accurately the current in the transmitting loop for two main reasons: 1) temperature instability of a small series resistor, 2) coupling effect between the voltmeter and other parts of the transmitting unit. However, the input current to the loop was

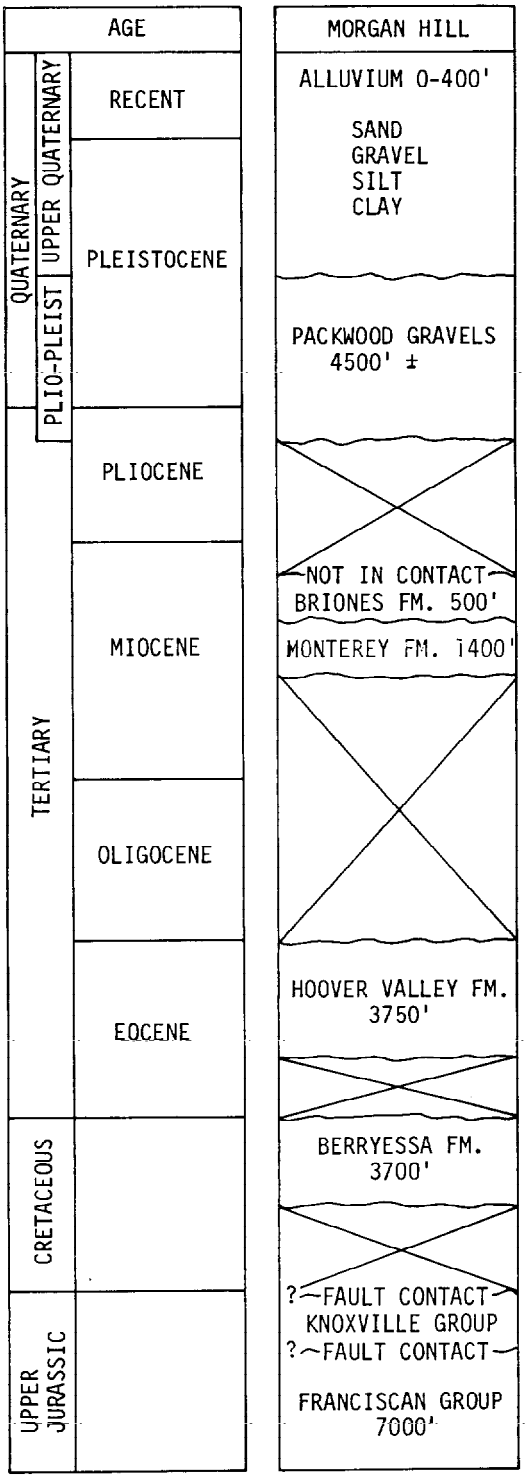

FIG. 2. Geologic column of Morgan Hill.

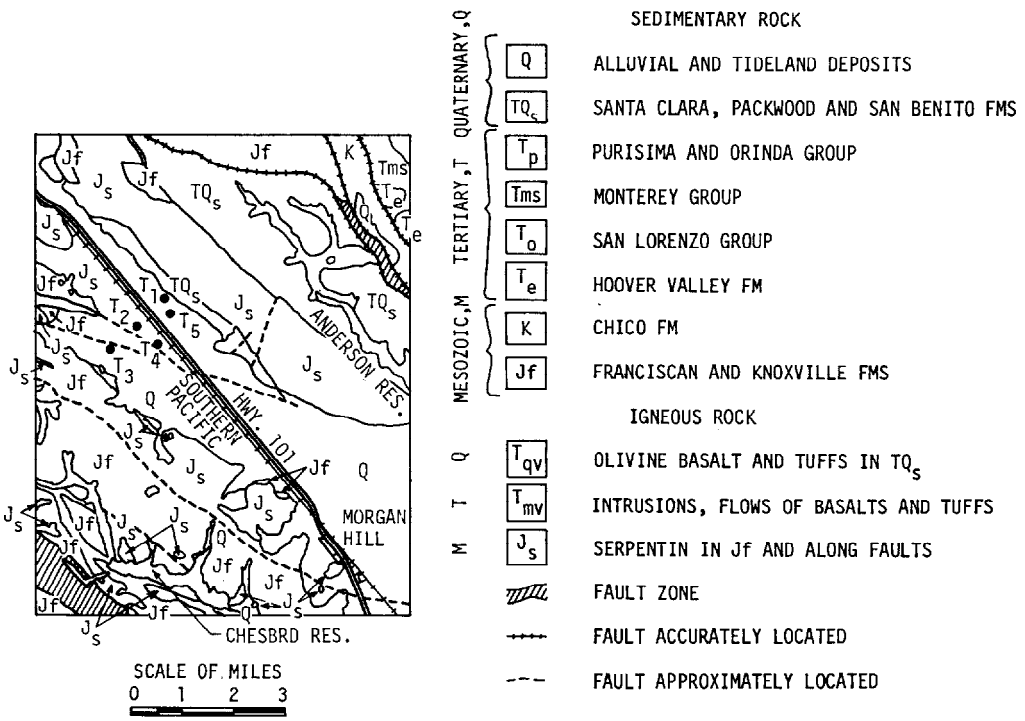

FIG. 3. Geologic map of Santa Clara Valley (Hill, 1955).

expected to vary from 1 amp to 10 amp over the desired range of frequency. It was observed that the ratio of signal to natural magnetic noise in the field was more than 40 db at the lower frequencies and more than 30 db at the higher frequencies with this input moment of the loop, when the transmitter-receiver distance was less than 700 ft and the gain of the preamplifier less than 100 ft. This indicates the adequacy of the designed sounding system for this study, as long as noise from other sources could be kept small.

DATA MEASUREMENTS AND REDUCTIONS

Measurements with this electromagnetic sounding system can be made of ten field quantities, i.e., moduli and phases of tangential electric field (E_θ), vertical magnetic field (H_z), horizontal magnetic field (H_r), wave tilt, tilt angle, and ellipticity. The last quantities are the polarization parameters of a polarization ellipse of the magnetic field vector. The polarization parameters of a polarization ellipse are described in Figure 6A, while Figure 6B shows a general behavior in the shape of the polarization ellipse for both sounding modes. The polarization parameters have the following advantages over the field components in data analysis:

1) independence of the input magnetic moment of the transmitting loop, which is troublesome to record accurately in the field,
2) ease and speed in taking data in the field,
3) better resolution in theoretical responses for layered models,
4) measurements do not require a reference voltage from the transmitter to the receiver; this feature eliminates ground loop problems and logistic difficulties.

Thus, the field data are to be analyzed in terms of the polarization parameters; knowledge of the input current to the transmitting loop is not needed.

Even though the system is capable of directly measuring the tilt-angle and ellipticity of the magnetic polarization ellipse, the bulk of the coil prohibits its accurate orientation. In order to obtain the polarization parameters indirectly, we choose to measure the modulus of the magnetic field vector (H_{45}) at an angle of 45 degrees with the surface toward the minor axis of the

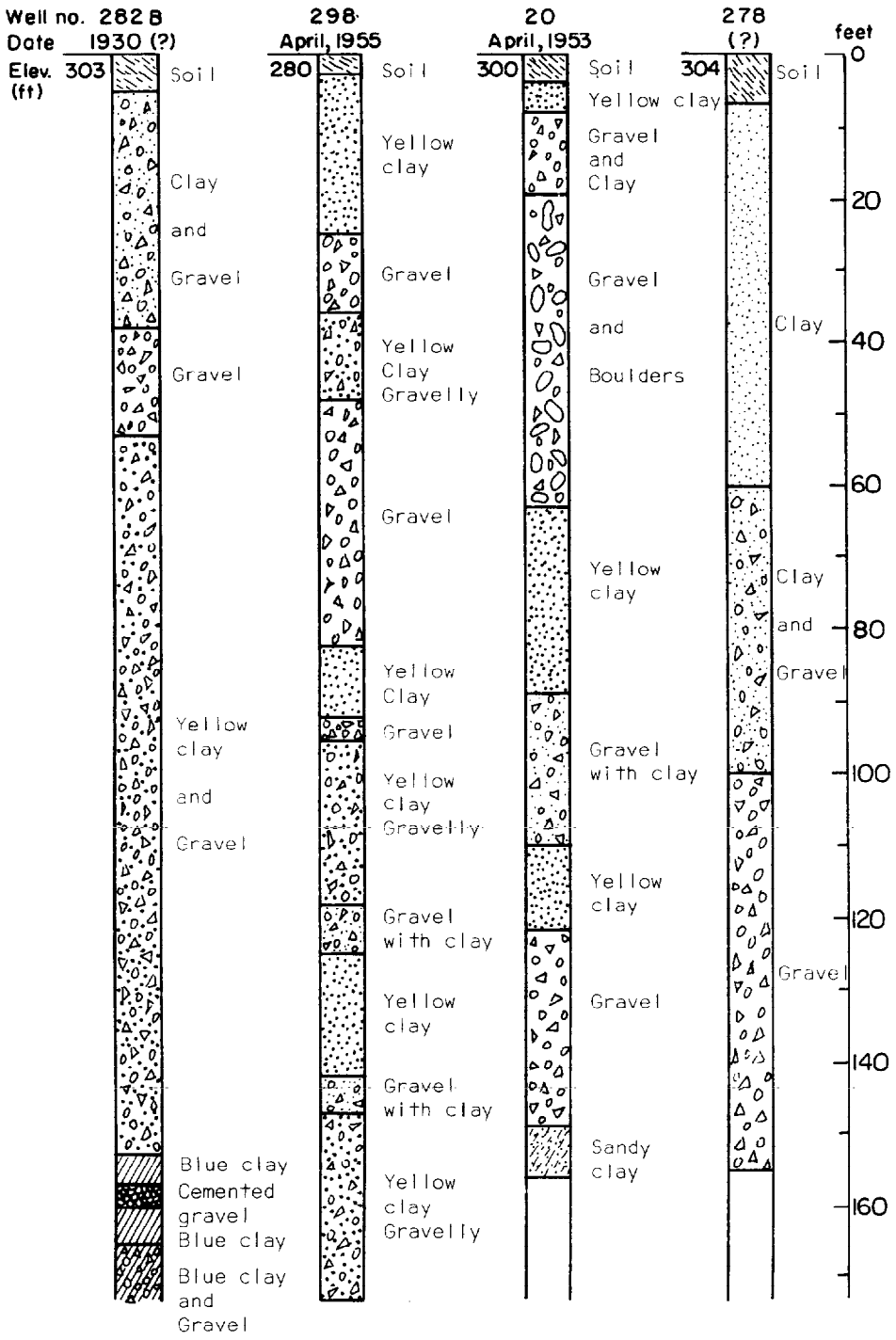

FIG. 4. Well data.

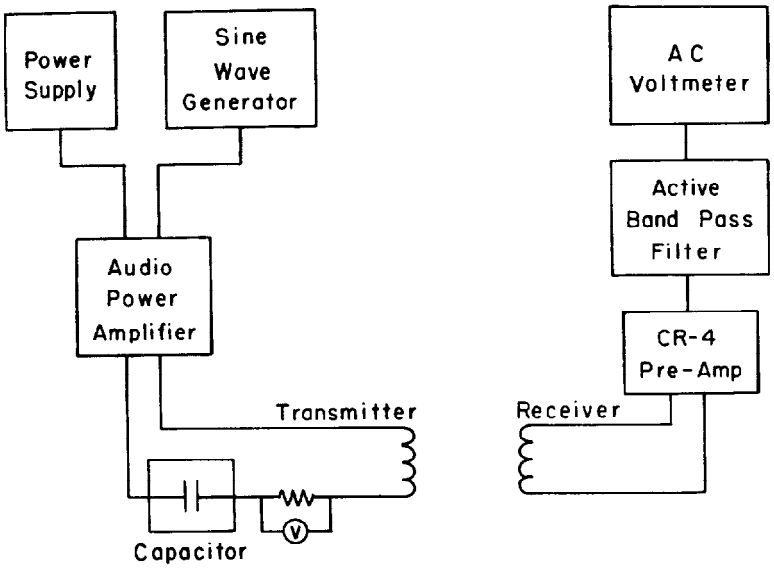

FIG. 5. Block diagram of sounding system.

polarization ellipse in addition to the moduli of H_r and H_z components. Referring to Figure 6A, we can calculate tilt angle, ellipticity, and wave tilt from the moduli of H_r, H_{45}, and H_z components with the following relations:

$$\text{Tilt Angle} = \alpha = \tan^{-1}\left(\frac{-B+(B^2+4A^2)^{1/2}}{2A}\right),$$

$$A = |H_r||H_z|\cos(\phi_r - \phi_z), \qquad B = |H_r|^2 - |H_z|^2, \tag{1}$$

$$\phi_r - \phi_z = \cos^{-1}\left\{\frac{1/2(|H_r|^2+|H_z|^2)-|H_{45}|^2}{|H_r||H_z|}\right\},$$

$$\text{Ellipticity} = H_2/H_1,$$

$$H_1 = |H_r\cos\alpha + H_z\sin\alpha|, \qquad H_2 = |-H_r\sin\alpha + H_z\cos\alpha|, \tag{2}$$

$$\text{wave tilt} = \frac{H_r}{H_z} = \left|\frac{H_r}{H_z}\right| e^{i(\phi_r-\phi_z)}, \tag{3}$$

where ϕ_r and ϕ_z are the phases of the H_r and H_z components, respectively.

A wise choice of transmitter-receiver distance is required to produce maximum responses over the frequency band specified with the given sounding system. Because the effect of displacement currents at the frequencies used in the surveyed area is negligible, theoretical studies (Ryu et al, 1970) show that this coplanar horizontal loop system, in general, has a maximum response to a layered structure over the range of induction numbers between 0.1 and 10.0, where the induction number θ is defined as the ratio of transmitter-receiver distance to skin depth which is computed with top layer resistivity. On this basis the transmitter-receiver distance r was chosen to be 400 ft (122 m) and 700 ft (214 m). When necessary, the results with $r=700$ ft can be translated to those with $r=400$ ft by use of the proportionality of the response to the induction number for the equivalent homogeneous half-space for any given frequency. The measurements at two different spacings should be diagnostic of the presence of lateral variations in resistivity and/or layer thickness and of inhomogeneities.

The transmitting loop was laid out at five sites. At each site there were two or three receiver-lines (Figure 1). The receiver occupied at least two different positions except for the line T_5-C. The moduli of H_r, H_{45}, and H_z components were measured normally at 14 frequencies between 200 hz and 10 khz. After the data were recorded and the transmitter turned off, the noise values of the three components were also collected. If necessary to maintain the signal to noise ratio

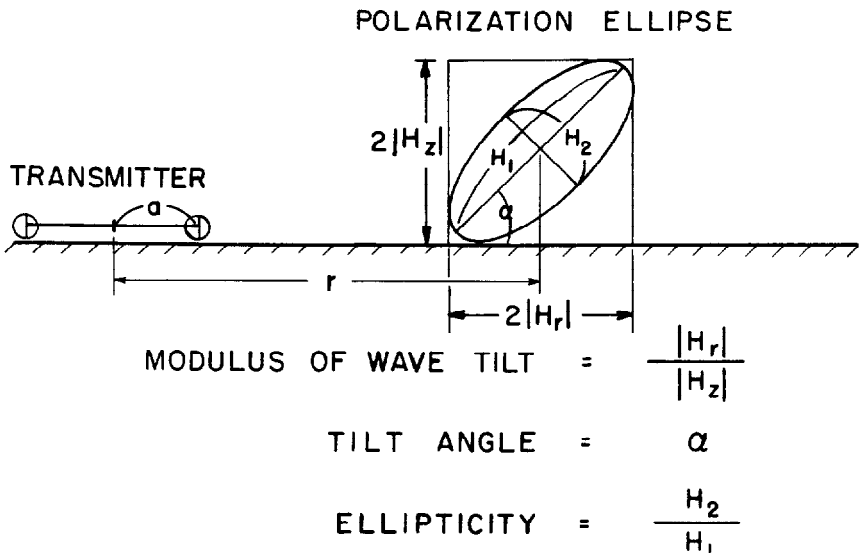

FIG. 6A. Parameters of magnetic polarization ellipse.

at more than 26 db, the readings were repeated. Then, the field data were computer processed to compute the values of the polarization parameters through equations (1), (2), and (3).

Many difficulties in the interpretation of the field data are expected due to the presence of more than two layers. Frischknecht (1967) indicates that partial curve-matching techniques, such as used in interpreting conventional resistivity data, would be unsuccessful in interpreting the electromagnetic frequency soundings. Exclusively, curve-fitting techniques are used for interpreting the field data through trial-and-error methods. A best-fit theoretical model at each transmitter site is chosen in such a way that it should match the obtained field curves for both tilt angle and ellipticity.

EXPERIMENTAL RESULTS

The representative tilt-angle responses shown in Figure 7 indicate different electrical structures over the five transmitter sites. In the figure, each symbol represents three characters. They indicate, in order, the location of the transmitting loop, a receiving line, and the distance in feet between the center of the transmitting loop and

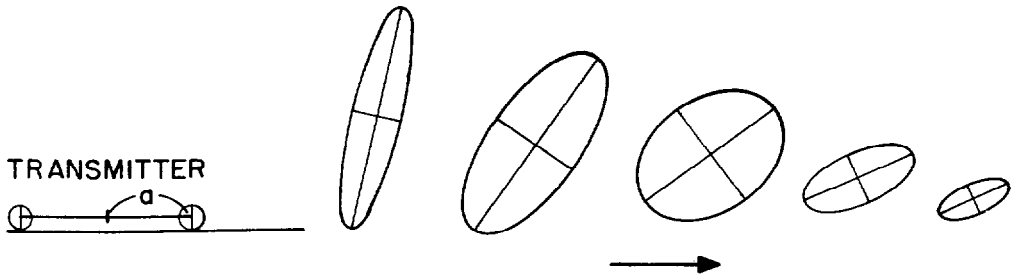

FIG. 6B. General behavior of magnetic polarization ellipse.

FIG. 8. Tilt-angle response from a homogeneous half-space.

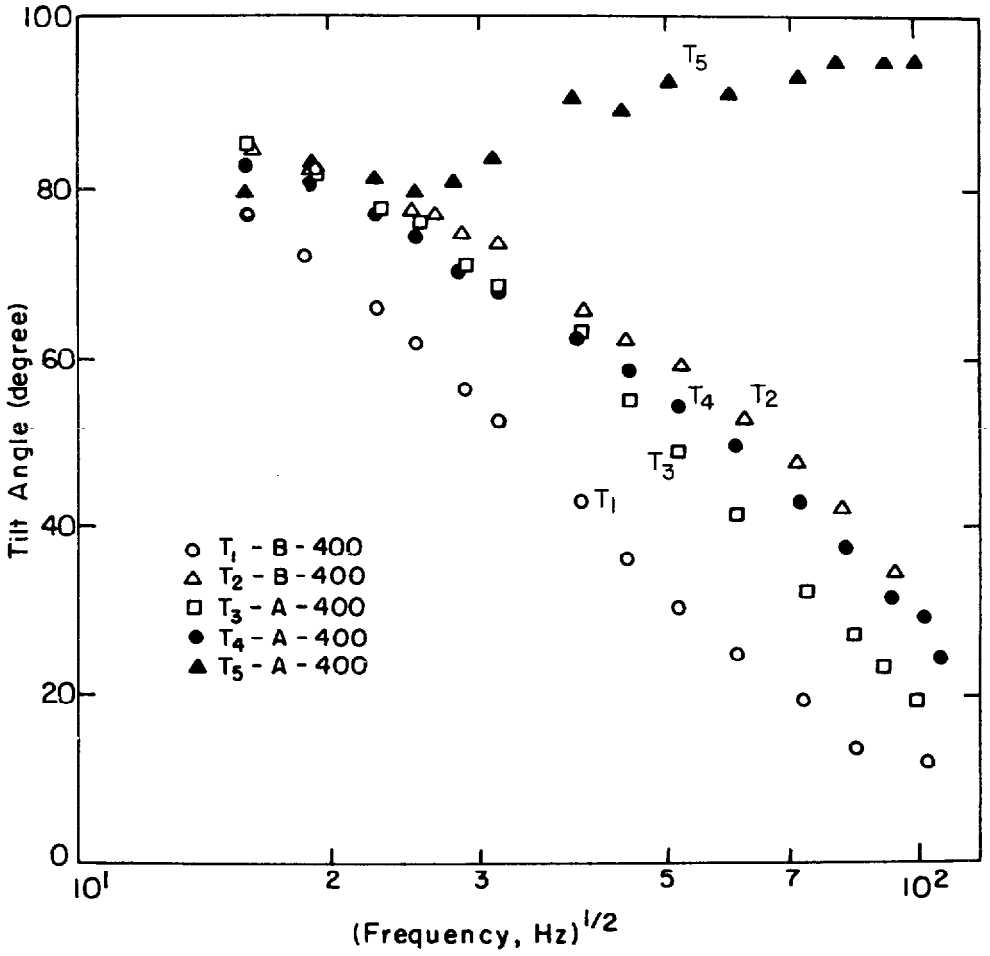

FIG. 7. Representative tilt-angle responses over five transmitter sites.

FIG. 9. Tilt-angle response at the site T_1.

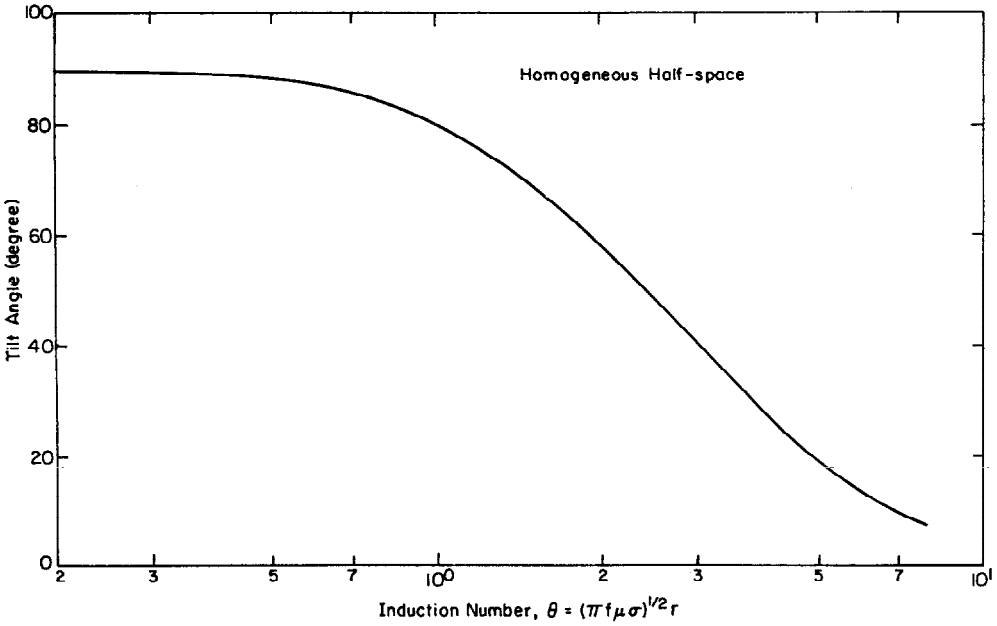
Homogeneous Half-space
Tilt Angle (degree)
Induction Number, $\theta = (\pi f \mu \sigma)^{1/2} r$

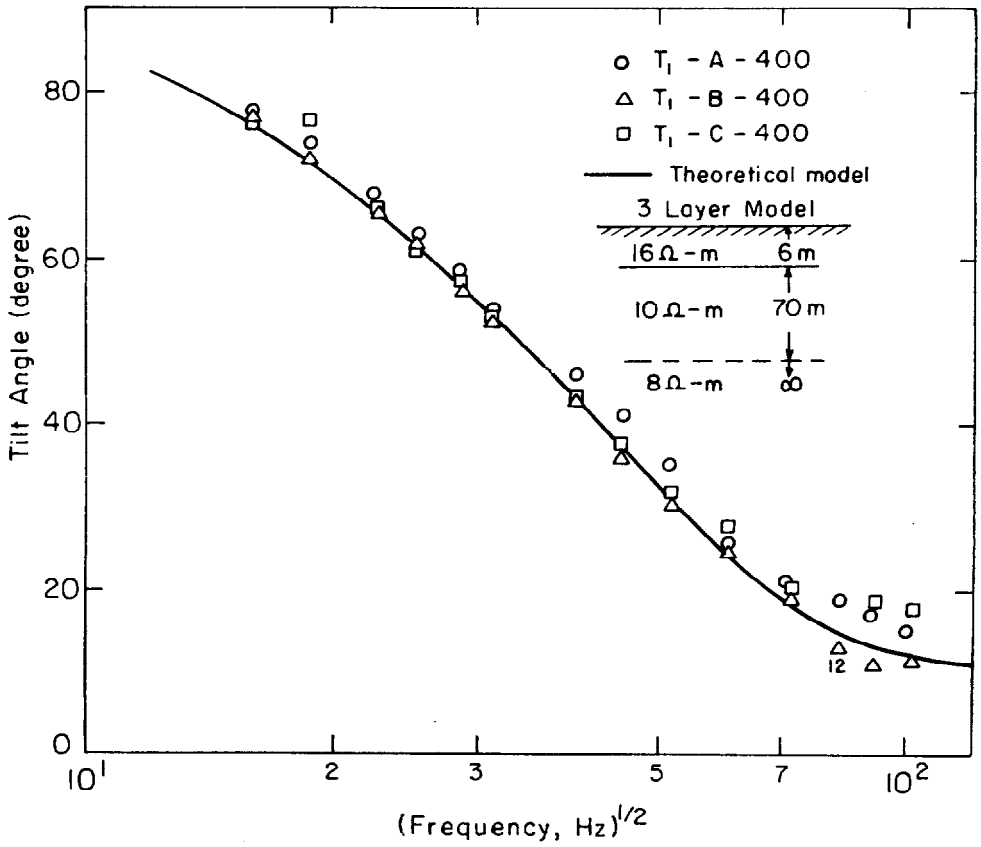
T_1 - A - 400
T_1 - B - 400
T_1 - C - 400
Theoretical model
3 Layer Model
16 Ω-m
6 m
10 Ω-m
70 m
8 Ω-m
Tilt Angle (degree)
(Frequency, Hz)$^{1/2}$

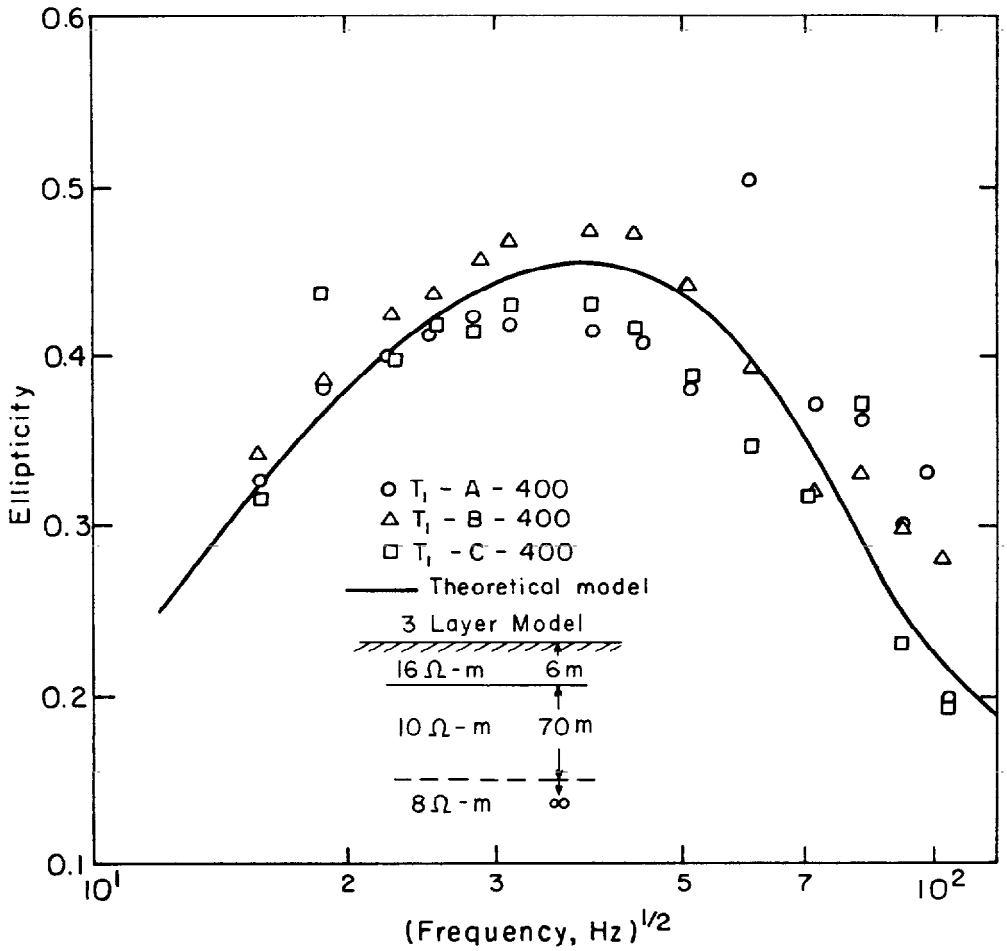

FIG. 10. Ellipticity response at the site T_1.

the receiver. All receiving lines of Figure 7 are perpendicular to the strike of the valley. The responses from the first four sites look, more or less, electrically horizontally layered on the basis of theoretical model studies, while the response at the fifth transmitter site suggests the presence of inhomogeneities along the receiving line. Hence, subsequent discussions are restricted to the first four sites.

Two deductions from comparison of theoretical curves for a layered half-space with those for a homogeneous half-space are pertinent. Figure 8 displays the tilt-angle versus induction number for a horizontal loop over a homogeneous earth. In studying similar curves for a layered half-space, we find that, with reference to the low-frequency asymptote, the tilt-angle versus either (frequency)$^{1/2}$ or induction number lies to the right of that shown in Figure 8, provided a resistive layer occurs between conductive layers in a three-layered half-space or provided the resistivity increases monotonically with depth. This is our first deduction. Secondly, a half-space in which the resistivity decreases monotonically with depth produces a tilt-angle versus either (frequency)$^{1/2}$ or induction number to the left of that shown in Figure 8.

With these deductions and the tilt-angle responses at the first four sites in Figure 7 in mind, we first note that the tilt-angle response at the first site T_1 is very similar to that due to a homogeneous, conductive half-space. However, resistivity decreasing with depth could possibly occur at site T_1. The other three sites must have

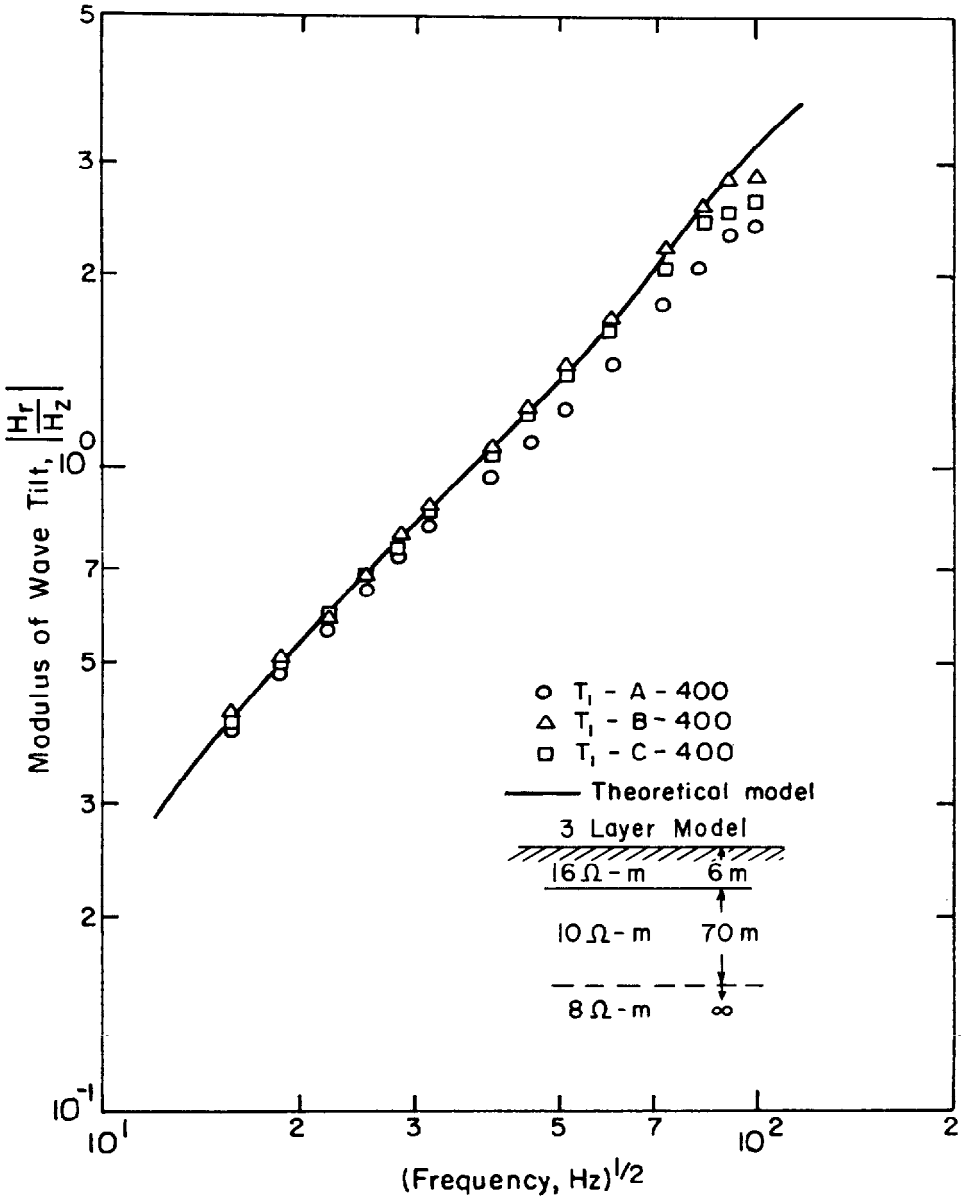

FIG. 11. Wave-tilt response at the site T_1.

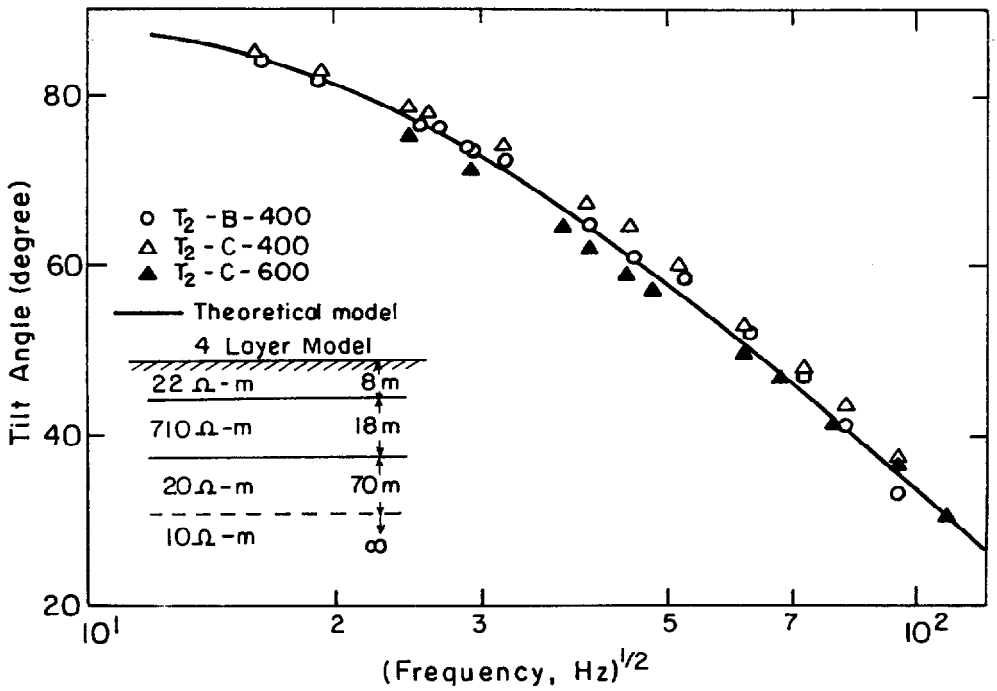

FIG. 12. Tilt-angle response at the site T_2.

an intermediate, resistive layer in between conductive layers or resistivity increasing with depth. We believe that an interpretation relying upon resistivity increasing with depth is unlikely. The curve shapes of tilt-angle responses at the transmitter sites T_2 and T_4, which are about 4500 ft apart along the strike direction of the valley, are shifted laterally along the axis of (frequency)$^{1/2}$. This fact may indicate that a slight change exists either in layer thicknesses with the same vertical resistivity distribution or in resistivities with the same layer-thicknesses at both sites.

Because none of the theoretical two-layered models already cataloged (Ryu et al 1970) for a variety of resistivity contrasts and thicknesses of the top layer closely fits any one of the responses, multilayered models, as expected from other sources, will be simulated with an assumption of no lateral electrical variation within an effective volume wherein any lateral variation violates the theoretical assumption of a horizontally layered half-space. In theoretical modelling, a prior knowledge of top-layer resistivity is essential. For simplicity in data reduction, the top-layer resistivity at each site was measured with conventional resistivity gear. However, in principle at least, it is possible to obtain the resistivities of all the layers from an electromagnetic sounding curve.

Figures 9 to 20 reveal the representative field responses of tilt-angle, ellipticity and the modulus of wave-tilt at the transmitter sites T_1, T_2, T_3, and T_4 in order. They also show the best-fit theoretical models for all sites. The polarization parameters are plotted, versus (frequency)$^{1/2}$, along two or more receiving lines perpendicular to each other in the figures. The scattering of data points can be attributed to lateral variations in resistivities and/or layer thicknesses, the presence of small pocket-type inhomogeneities, unstable input current to the transmitting loop during measuring period of all three components, nonlinearity of system response of the receiving unit, the misorientation of the receiving coil from desired angles, man-made noise, or instrumental errors and/or noises.

VARIABILITY OF CHOSEN ELECTRICAL STRUCTURE

Figure 21 summarizes the electrical layerings of the surveyed area. It is wise to question the variability of chosen structure parameters P_i within the permissible ranges of polarization

parameters. As an example, let us consider a 4-layered structure in terms of the response of tilt-angle. Then, we can write the tilt-angle response at a frequency f as:

$$\text{Tilt-Angle, } T_f = T_f(h_1, h_2, h_3, \rho_1, \rho_2, \rho_3, \rho_4),$$

where h_i and ρ_i represent the thickness and resistivity of the ith layer respectively.

The variation of the tilt-angle is:

$$\Delta T_f = \frac{\partial T_f}{\partial h_1}\Delta h_1 + \frac{\partial T_f}{\partial h_2}\Delta h_2 + \frac{\partial T_f}{\partial h_3}\Delta h_3 + \frac{\partial T_f}{\partial \rho_1}\Delta \rho_1 + \frac{\partial T_f}{\partial \rho_2}\Delta \rho_2 + \frac{\partial T_f}{\partial \rho_3}\Delta \rho_3 + \frac{\partial T_f}{\partial \rho_4}\Delta \rho_4.$$

To simplify the problem, we will vary one parameter, p, holding other parameters constant, where p can be either h_i or ρ_i. Then, we can simply write a partial derivative as:

$$\frac{\partial T_f}{\partial p} \cong \frac{\Delta T_f}{\Delta p}.$$

The variation ΔT also varies over the desired range of frequency with a given Δp. Theoretically the response at higher frequencies from the upper layer has a large variation for a given change in either resistivity or thickness of the top layer, while the lower layer affects the response at lower frequencies, where the response has a small variation. Thus, the permissible ΔT should be varied, depending on a chosen parameter. Then the variation $\Delta p_i (i = 1, \ldots, 7)$ is to be found with a permissible ΔT at a particular frequency,

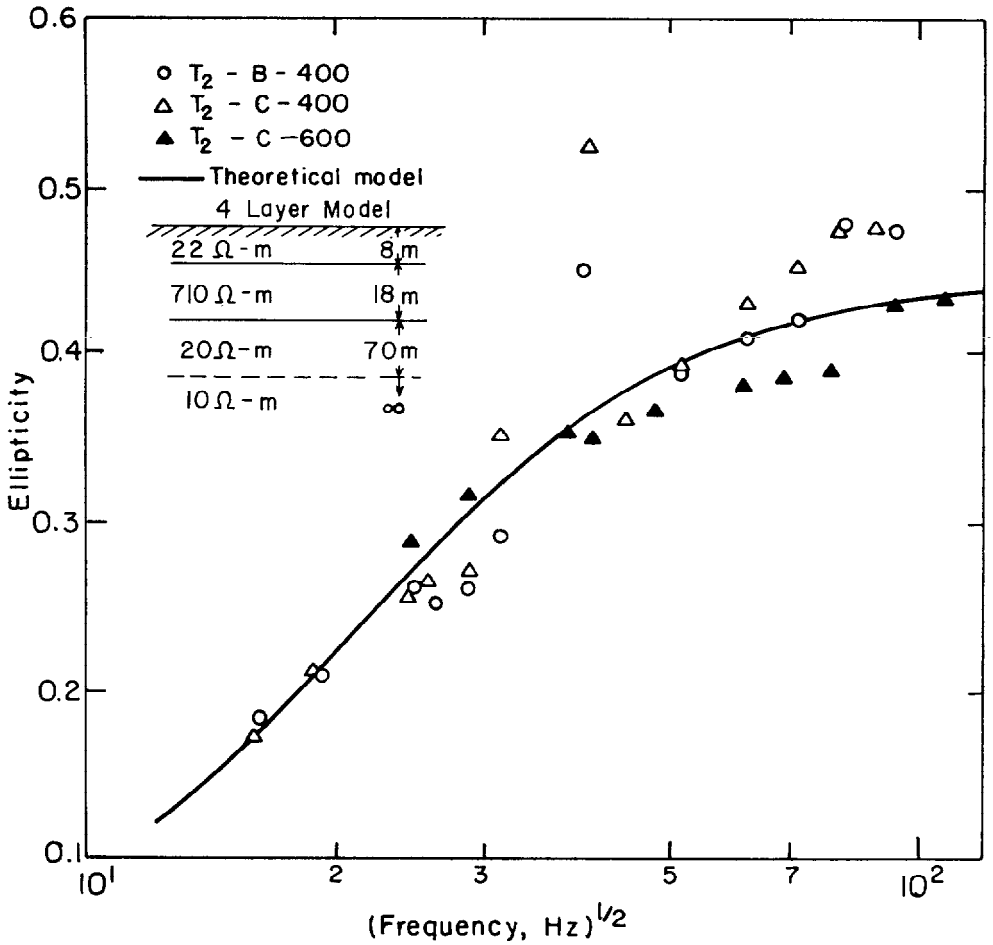

FIG. 13. Ellipticity response at the site T_2.

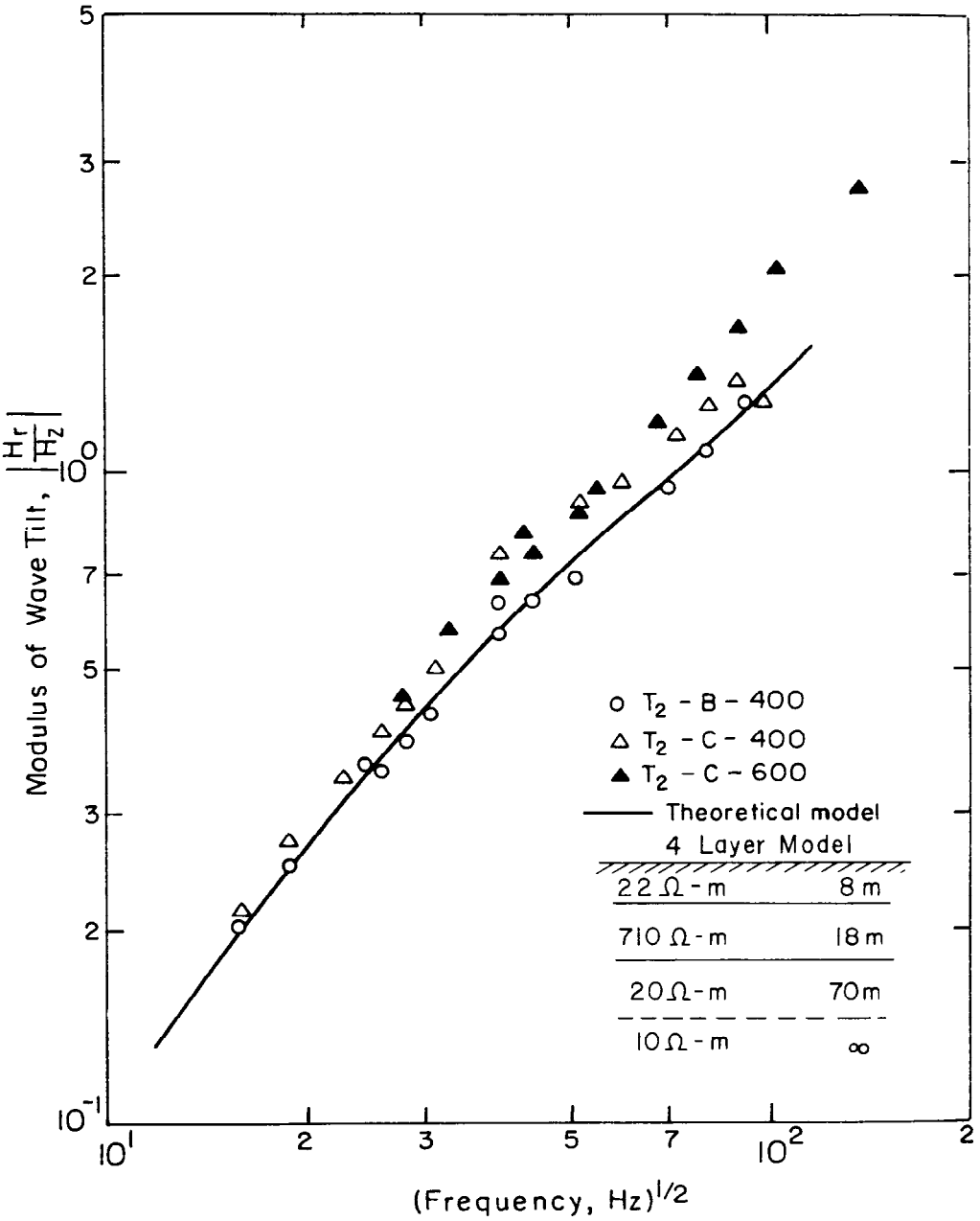

FIG. 14. Wave-tilt response at the site T_2.

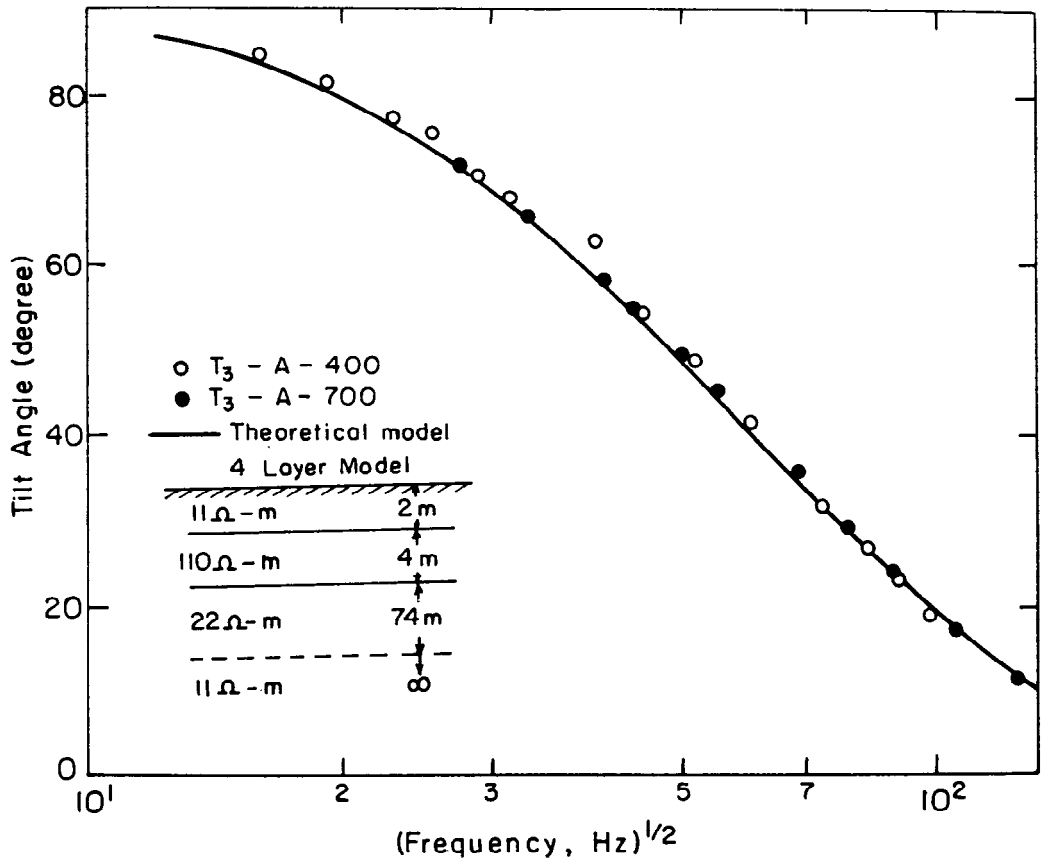

FIG. 15. Tilt-angle response at the site T_3.

at which ΔT is maximum with a specified Δp_i.

For example, we choose the theoretical model for the transmitter site T_2. The general implications of the results can be extended to those of other sites. Computations for this model were made at frequencies of 200 hz, 500 hz, 1 khz, 2 khz, 5 khz, and 10 khz.

Figures 22 and 23 show the variations of layer thicknesses and of resistivities, respectively, plotted against the variation of tilt-angle for the model T_2. These figures show that the tilt-angle is not sensitive to the depth to the bottom discontinuity and the resistivities of the second resistive layer and the bottom layer. The current is flowing mostly through the first and third conductive layers, but not through the intermediate, resistive layer. As a result, the resistivity of the resistive layer makes a small contribution to the response, while its thickness makes a large difference to the contribution from the third layer It is concluded that the bottom discontinuity is uncertain, but the response clearly reveals the presence of an intermediate, resistive layer in between conductive layers. The upper and lower limits of the parameters are tabulated in Table 1 with the permissible variations of tilt-angle specified. The permissible ranges of tilt-angle variation for each parameter are chosen with regard to measuring accuracy as well as the frequency band, over which the parameter has a maximum contribution to the response. The qualitative ratings of sensitivity to the response are given in the last column of the table.

GEOLOGICAL INTERPRETATION OF RESULTS

An electrical section across the valley along the line B—B′ (Figure 1) is drawn in Figure 24 from

Table 1. Sensitivity ratings

Parameter		Frequency	Δ Tilt-angle permissible	Minimum	Chosen value	Maximum	Sensitivity rating
Thickness (meter)	1st Layer	10 khz	±2.0	6.0 m	8.0 m	10.0 m	Good
	2nd Layer	5 khz	±2.0	15.5	18.0	21.0	Good
	3rd Layer	500 hz	±1.0	44.0	70.0	160.0	Fair
Resistivity (ohm-m)	1st Layer	10 khz	±2.0	19.5 Ω-m	22.0 Ω-m	25.7 Ω-m	Good
	2nd Layer	10 khz	±1.0	300	710	>5000	Poor
	3rd Layer	2 khz	±2.0	17.0	20.0	24.5	Good
	4th Layer	200 hz	±1.0	5.0	10.0	<25.0	Poor

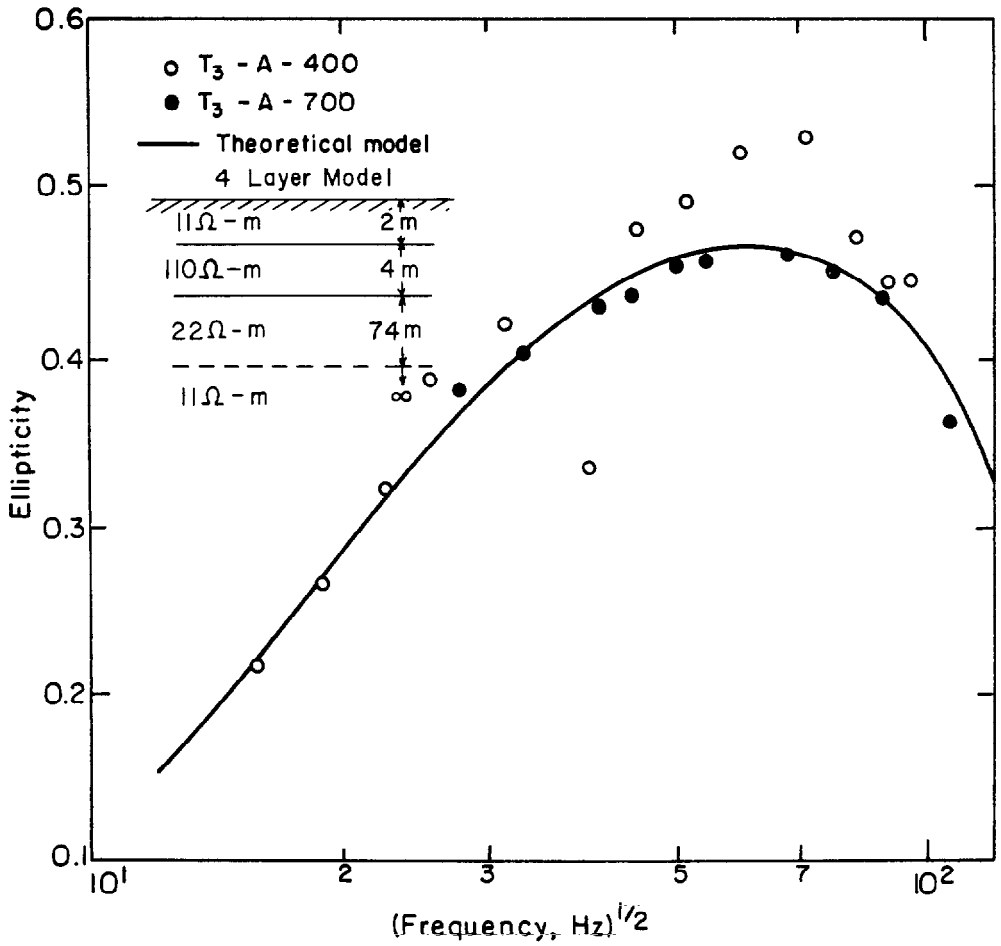

FIG. 16. Ellipticity response at the site T_3.

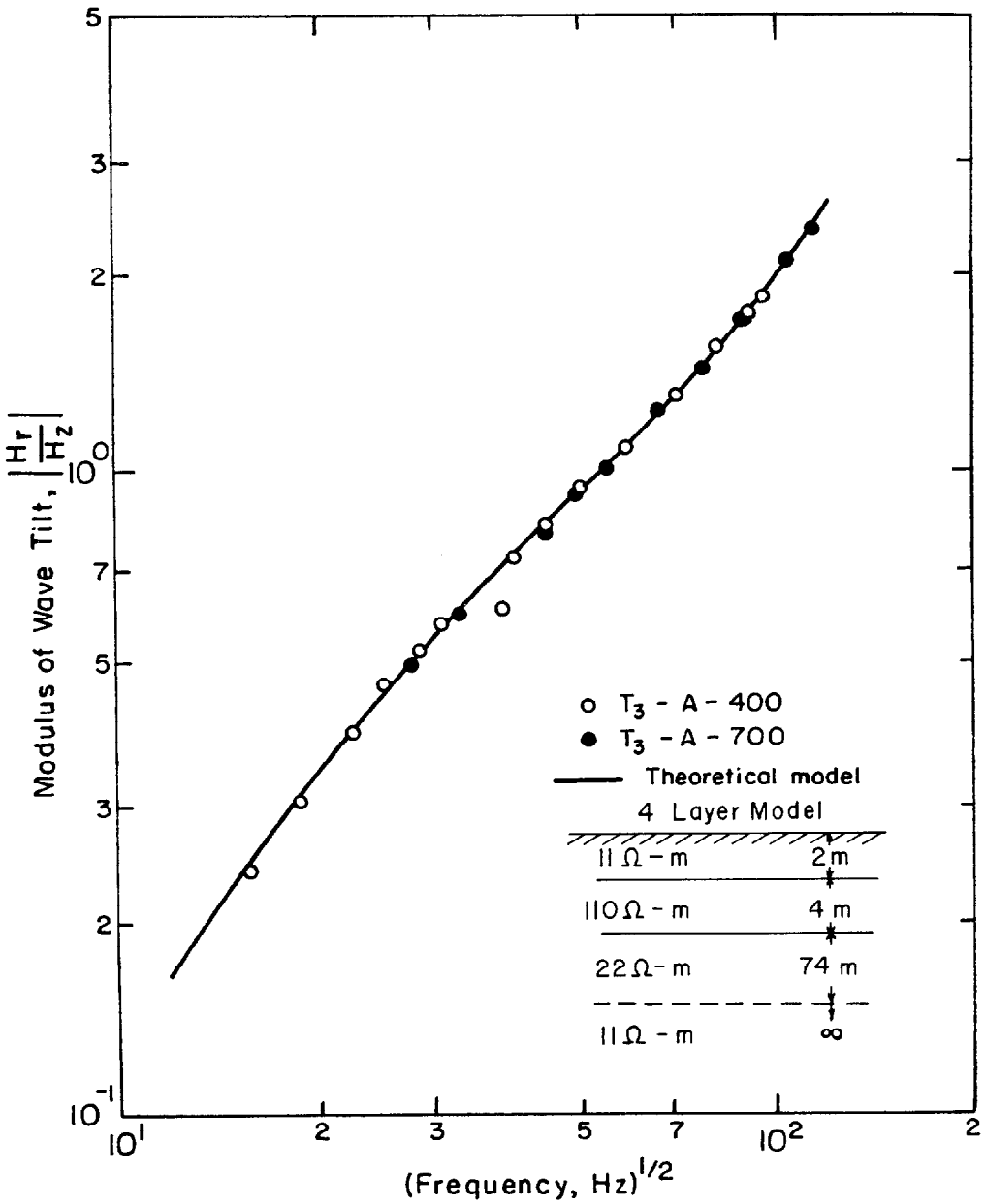

FIG. 17. Wave-tilt response at the site T_3.

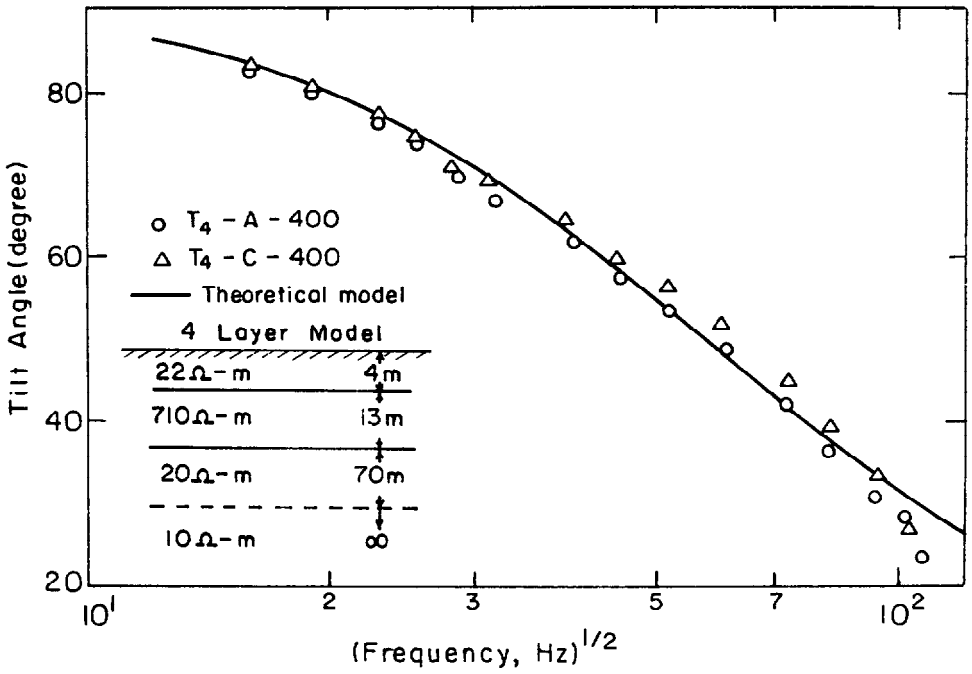
Tilt Angle (degree)
80
60
40
20
10^1
2
3
5
7
10^2
(Frequency, Hz)$^{1/2}$
o T_4 - A - 400
△ T_4 - C - 400
Theoretical model
4 Layer Model
22Ω-m
4m
710Ω-m
13m
20Ω-m
70m
10Ω-m
∞

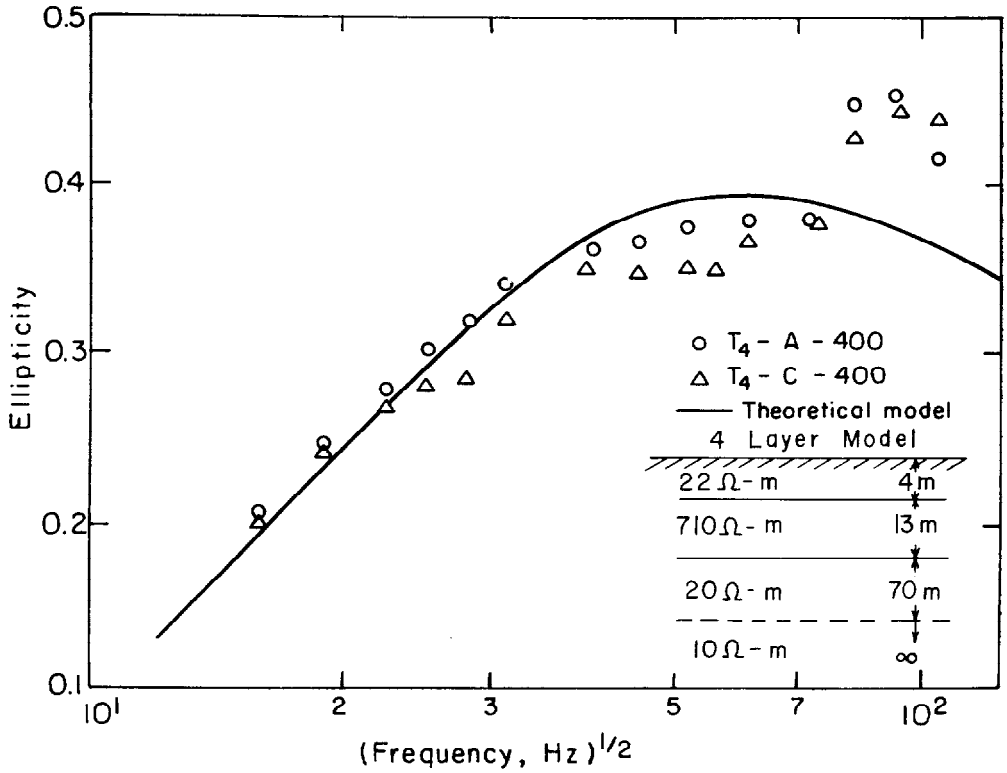
Ellipticity
0.5
0.4
0.3
0.2
0.1
10^1
2
3
5
7
10^2
(Frequency, Hz)$^{1/2}$
o T_4 - A - 400
△ T_4 - C - 400
Theoretical model
4 Layer Model
22Ω-m
4m
710Ω-m
13m
20Ω-m
70m
10Ω-m
∞

FIG. 18. Tilt-angle response at the site T_4.

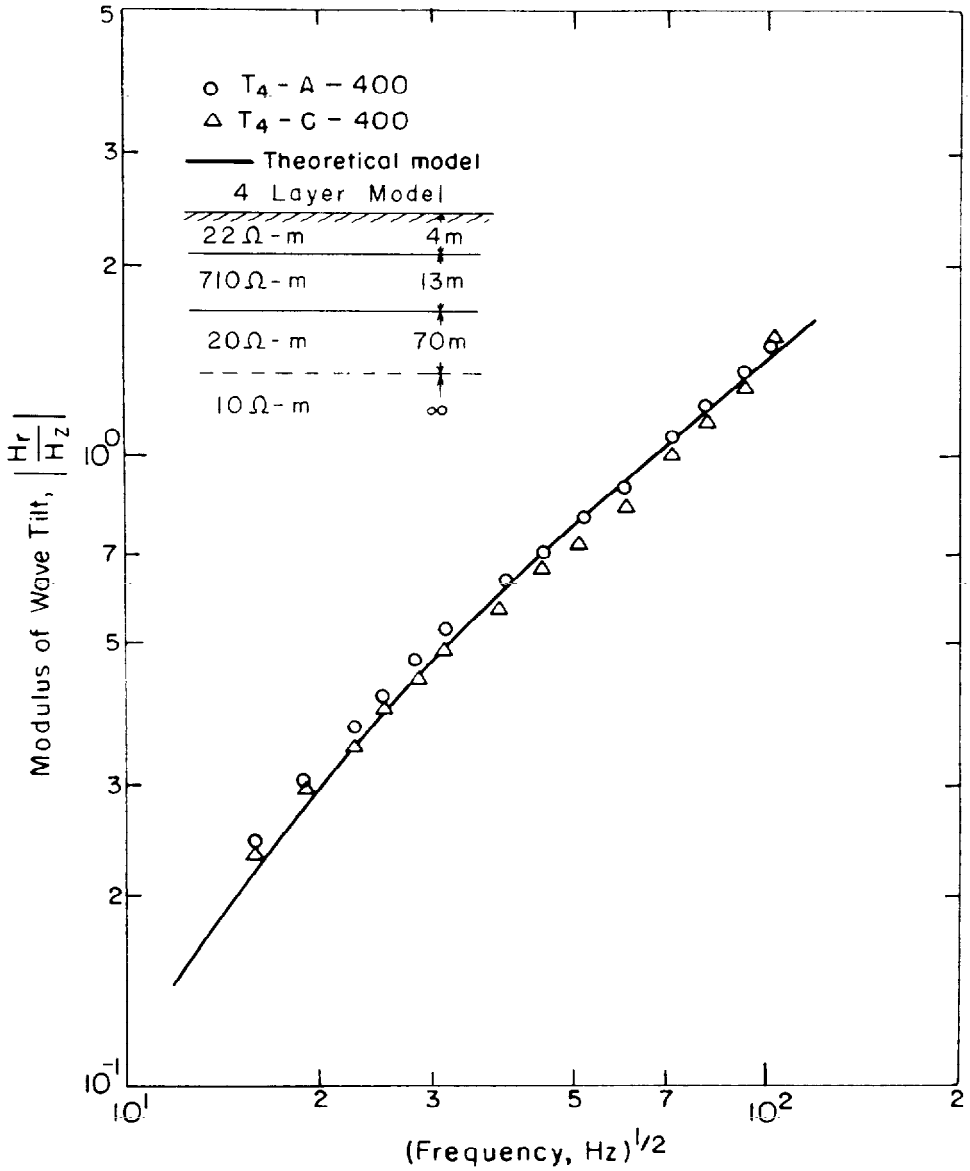

FIG. 20. Wave-tilt response at the site T_4.

FIG. 19. Ellipticity response at the site T_4.

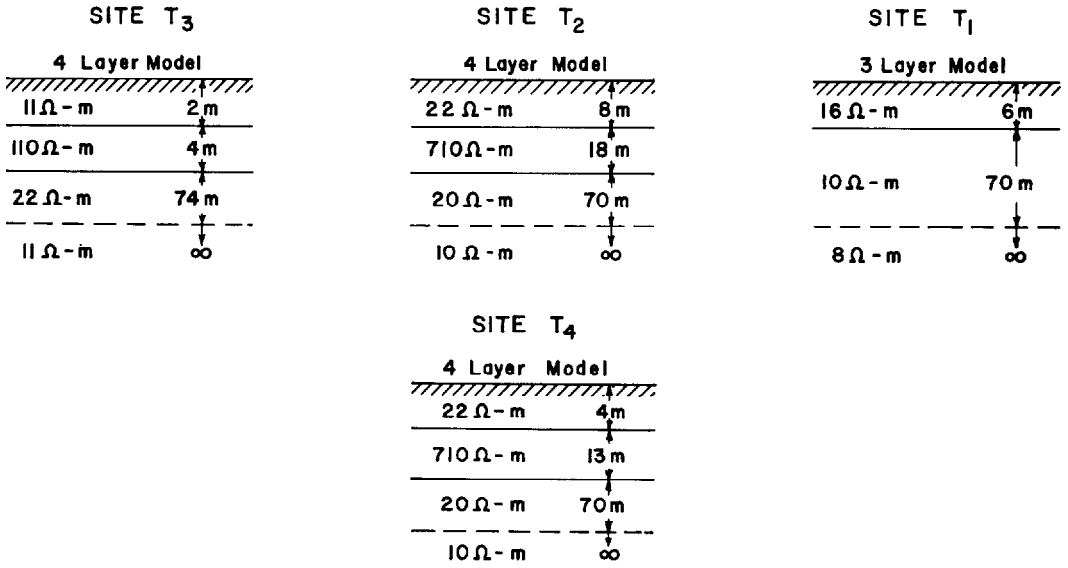

FIG. 21. Summary of electrical layerings over the surveyed area.

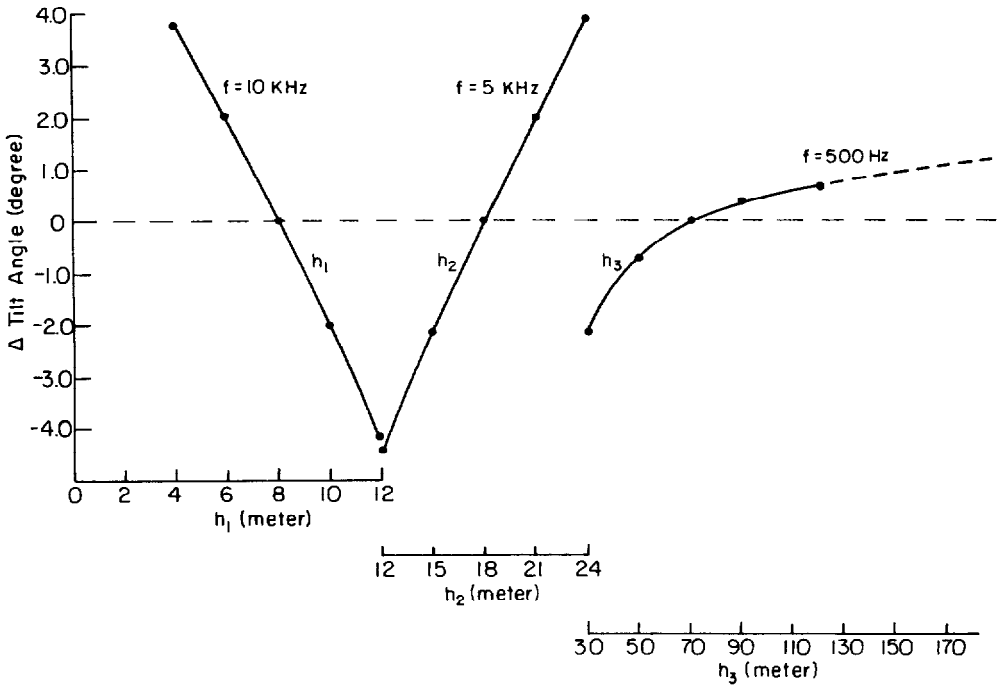

FIG. 22. Variation of layer thicknesses plotted against variation of tilt-angle for the model T_2.

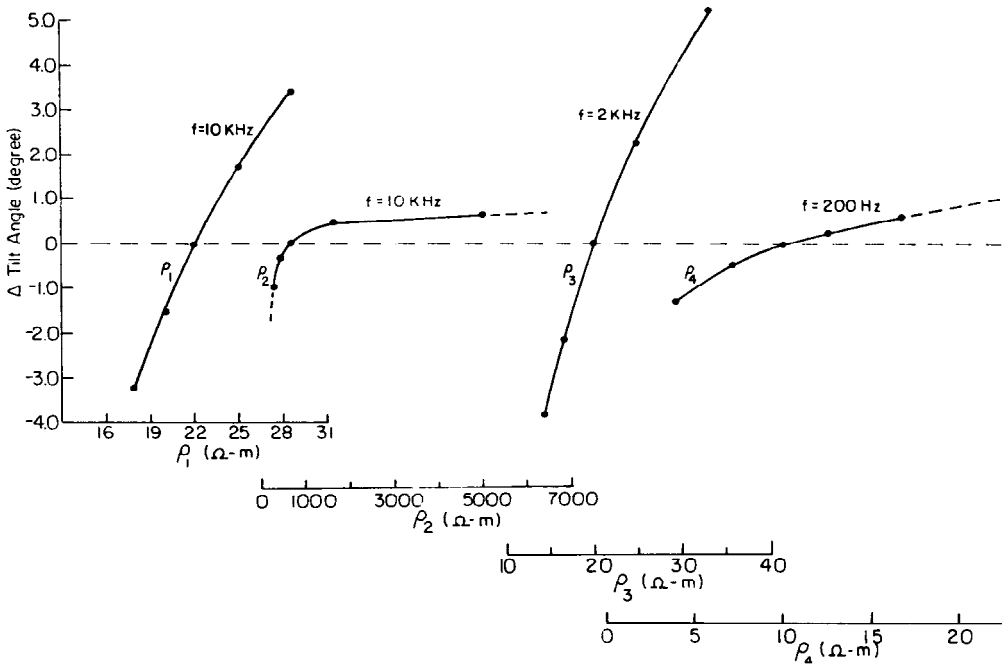

FIG. 23. Variation of resistivities plotted aginst variation of tilt-angle for the model T_2.

the interpretation of the experimental data. A highly resistive, intermediate layer with a thickness of about 18 m is located at a depth of 8 m below the transmitter site T_2 in the middle of the valley and pinches out toward the edges of the valley. The bottom discontinuity between unconsolidated sediments and bedrock is obscure in the responses. A successful deduction of depth to the bedrock requires lowering frequency about a decade.

The obtained electrical section is in good agreement with the data from well 20 and well 298 (Figure 4), which are 300 ft off from the profile, as well as with the geologic section shown in Figure 25 along line C–C′ (Figure 1), which is about 2000 ft away from line B–B′. The geologic section was supplied by the Water Conservation District, Santa Clara Valley and was based on resistivity soundings and other sources. The conductive top-layer consists of soil, clay, and a little gravel. The second layer with a thickness of about 100 m below the transmitter site T_1 represents a block of still quite conductive sediments of Tertiary or early Quaternary age. Toward the western edge of the valley, a second layer of gravels and boulders occurs at a variable depth and with a variable thickness, yielding a permeable stratum for groundwater recharge. This layer is over the third layer of old alluvium, surrounded by the bedrock.

CONCLUSION

The electrical discontinuities deduced from the computer-processed data of the electromagnetic depth sounding experiment carried out across Santa Clara Valley, California are consistent with well data and the geologic section based on conventional resistivity soundings. The interpretation of field data was made in terms of the polarization parameters of the magnetic field vector via trial-and-error curve matching techniques. The polarization parameters chosen were tilt-angle, ellipticity, and the modulus of wave-tilt, which are independent of the input current to the transmitting loop. The results clearly reveal an intermediate, highly resistive layer, which is a permeable stratum for groundwater recharge. It can be concluded that a portable electromagnetic sounding system, measuring only tilt-angle and ellipticity, should easily

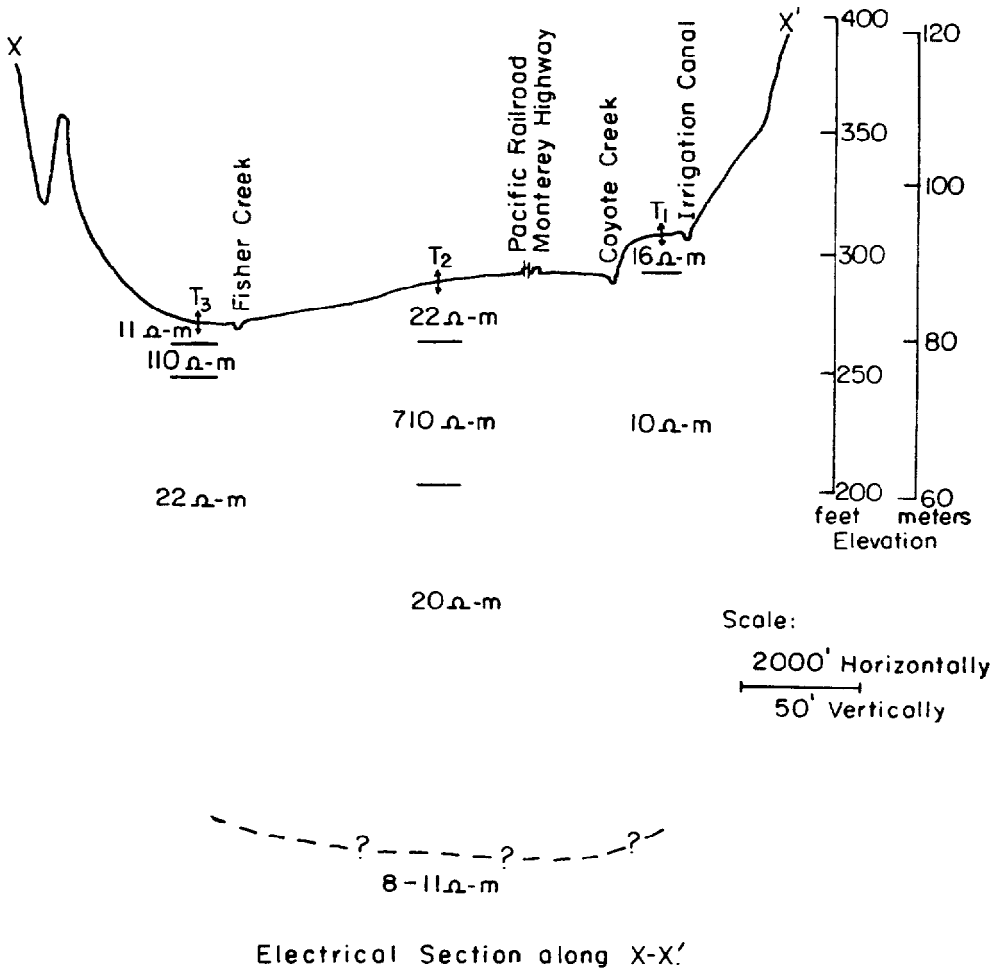

FIG. 24. An electrical section across the valley along the line X–X'.

locate highly resistive gravel deposits for rechargeable aquifers, provided conductive beds bound it on top and bottom.

This experiment indicates that an electromagnetic depth sounding system can serve the same purpose as a conventional resistivity system. In addition, it is theoretically obvious that the former should overcome the main problem of the latter: a difficulty in injecting current into a highly resistive surface layer. Additional potential advantages of an electromagnetic system over a resistivity system include lower survey cost and higher resolution.

ACKNOWLEDGMENTS

The study was supported by the Water Resources Center of the University of California and by the Office of Water Resources Research, United States Department of the Interior, which provided "matching funds" under Public Law 88-79.

The authors would like to express their appreciation to the U.S. Naval Shipyard, Mare Island, California, and to Kennecott Exploration Services, Inc., Salt Lake City, Utah, for providing equipment. Thanks are due to Mr. Leo M. Page and Mr. John H. Clark of the Santa Clara Water

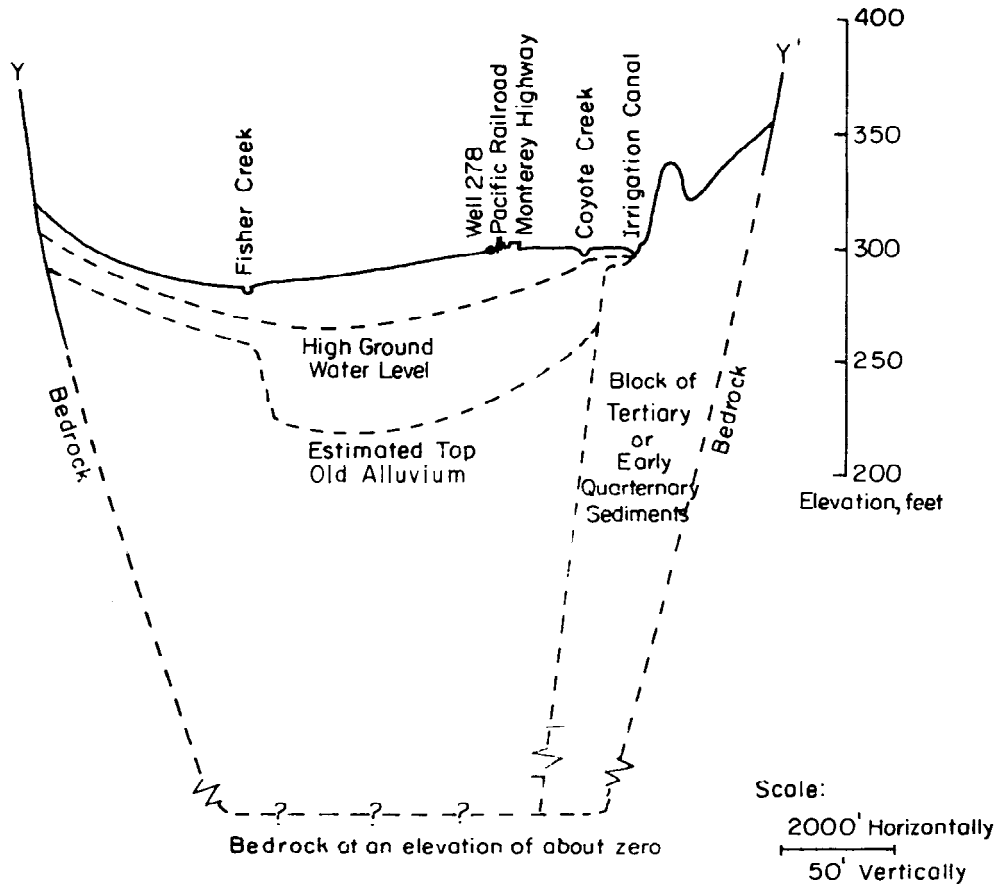

FIG. 25. A geologic section across the valley along the line Y–Y', supplied by Santa Clara Water Conservation District.

Conservation District for supplying geologic information over the surveyed area and arranging the field sites with land-owners.

Mr. Jack Mego in the Engineering Geoscience Laboratory maintained the system electronics in the field. This project could not have been successful without the help of graduate students in engineering geoscience, University of California, Berkeley, during various stages of the work. Among them are Messrs. W. Glenn, A. Kalra, A. Dey, D. Trussell, and R. Zelwer. Also the authors particularly thank Dr. G. W. Hohmann and Mr. J. C. Coggon for their valuable suggestions in the field operation as well as in data processing.

REFERENCES

Bodmer, R., Ward, S. H., and Morrison, H. F., 1968, On induced electrical polarization and groundwater: Geophysics, v. 33, p. 805–821.

Breusse, J. J., 1963, Modern geophysical methods for subsurface water exploration: Geophysics, v. 28, p. 633–657.

Dey, A., and Ward, S. H., 1970, Inductive sounding of a layered earth with horizontal magnetic dipoles: Geophysics, v. 35, p. 660–703.

Duckworth, K., 1970, Electromagnetic depth sounding applied to mining problems: Geophysics, v. 35, p. 1086–1098.

Frischknecht, F. C., 1967, Fields about an oscillating magnetic dipole over a two-layer earth and application to ground and airborne electromagnetic survey: Q. Colo. Sch. of Mines, v. 72, no. 1.

Hill, C. A., 1955, Santa Clara Valley Investigation: Bulletin No. 7, California, State Water Resources Board.

Hohmann, G. W., Kintzinger, P. R., Van Voorhis, G. D., and Ward, S. H., 1970, Evaluation of the measurement of induced electrical polarization with an inductive system: Geophysics, v. 35, p. 901–915.

Inonye, G. T., Bernstein, H., and Gaal, R. A., 1969, Electromagnetic depth sounder: Unpublished manuscript, TRW Systems, Redondo Beach, California.

Keller, G. V., and Frischknecht, F. C., 1966, Electrical methods in geophysical prospecting: New York, Pergamon Press.

Patra, H. P., 1967, Some studies on geoelectric sounding in engineering and hydro-geologic problems: Ph.D. thesis, IIT India.

Poland, J. F. and Green, J. H., 1962, Subsidence in the Santa Clara Valley, California, a progress report: USGS, Water Supply Paper no. 1619C.

Ryu, J., Morrison, H. F., and Ward, S. H., 1970, Electromagnetic fields about a loop source of current: Geophysics, v. 35, p. 862–896.

Sumi, F., 1965, Prospecting for non-metallic minerals by induced polarization: Geophys. Prosp., v. 13, p. 603–616.

Vacquier, V., Holmes, C. R., Kintzinger, P. R., and Lavergne, M., 1957, Prospecting for ground water by induced electrical polarization: Geophysics, v. 22, p. 660–687.

Vanyan, L. L., 1967, Electromagnetic depth sounding: selected and translated by Keller, G. V., New York, Consultants Bureau.

Zohdy, A. A. R., 1964, Earth resistivity and seismic refraction investigations in Santa Clara County, California: Ph.D. Thesis, Stanford University, Palo Alto, California.